Genetic Algorithm-Assisted Combinatorial Search for New Blue Phosphors in a (Ca,Sr,Ba,Mg,Eu)$_x$B$_y$P$_z$O$_\delta$ System

Yu Sun Jung,[†] Chandramouli Kulshreshtha,[†] Ji Sik Kim,[‡] Namsoo Shin,[§] and Kee-Sun Sohn*[,†]

Department of Materials Science and Metallurgical Engineering, Sunchon National University, Chonnam 540-742, Korea, Department of Advanced Materials Engineering, Sangju National University, 742-711 Kyeongbuk, Korea, and Beamline Division, Pohang Accelerator Laboratory, 790-784 Kyungbuk, Korea

Received April 9, 2007. Revised Manuscript Received August 29, 2007

Genetic algorithm-assisted combinatorial chemistry (GACC) was implemented to search for new blue phosphors in seven cation systems, including CaO, MgO, BaO, SrO, B_2O_3, P_2O_5, and Eu_2O_3. The GACC process was followed by a series of fine-tuning processes based on conventional high-throughput screening employing quaternary and ternary libraries, to pinpoint promising compositions. GACC was found to be useful as a preliminary step for final screening. This series of processes involving computations and actual syntheses led us to $(Sr_{1-x-y}Ca_xBa_y)_2P_2O_7:Eu^{2+}$ ($0.32 < x < 0.72$, $y < 0.04$) phosphors. It was found that the boron addition played a significant role in enhancing the luminance but it was completely evaporated during the synthesis, and an excessive amount of alkali earth elements was essential for better luminescence. The luminance of $(Sr_{1-x-y}Ca_xBa_y)_2P_2O_7:Eu^{2+}$ ($0.32 < x < 0.72$, $y < 0.04$) phosphors reached 70% of a commercially available BAM phosphor at 254 nm excitation. The color chromaticity was in the deep blue region, $x = 0.15$, $y = 0.05$. The structure of these phosphors was found to be $Sr_2P_2O_7$ (*Pnma*, 62), but the luminescent property was far better than the $Sr_2P_2O_7:Eu^{2+}$ phosphor.

1. Introduction

$Sr_6BP_5O_{20}:Eu^{2+}$ (SBP) in an $I\bar{4}c2$ symmetry has recently been identified as a good phosphor,[1−3] the luminance of which was as high as 280% of a commercially available $BaMgAl_{10}O_{17}:Eu^{2+}$ (BAM) phosphor at UV and VUV excitation and much more thermally stable than BAM. Nonetheless, SBP is not practically useful as a blue phosphor because the color chromaticity is not acceptable.[1,2] One plausible approach to developing a promising blue phosphor, the color chromaticity and luminance of which should be acceptable, would be a combinatorial screening in the Eu^{2+}-doped (Ca,Sr,Ba,Mg)$_x$B$_y$P$_z$O$_\delta$ system. Among those exhibiting blue emission of high luminance at UV/VUV excitation, several candidates have attracted interest in the alkali earth phosphate, halophosphate, and borophosphate system. For example, $A_2P_2O_7:Eu^{2+}$, $A_3(PO_4)_3:Eu^{2+}$, $A_5(PO_4)_3Cl:Eu^{2+}$, and SBP (A = alkali earth elements) have been well-known as traditional blue phosphors, but their luminescence inclines toward deep blue, ultraviolet, or greenish-blue.[4−6] A quantitative structure property relationship (QSPR) deserves to be obtained in the Eu^{2+}-doped (Ca,Sr,Ba,Mg)$_x$B$_y$P$_z$O$_\delta$ system to discover new blue phosphors that exceed the traditional blue phosphors in terms of the color chromaticity and luminance. This means that the luminescent property should be expressed as a function of composition in the composition range of concern. The aim of the present investigation is to search for new blue phosphors in the Eu^{2+}-doped (Ca,Sr,Ba,Mg)$_x$B$_y$P$_z$O$_\delta$ system by employing a strategy involving high-throughput combinatorial chemistry and a computational evolutionary optimization based on genetic algorithms.

There could be a very large number of potential candidates for blue phosphors in the Eu^{2+}-doped (Ca,Sr,Ba,Mg)$_x$B$_y$P$_z$O$_\delta$ system, which involves seven cation oxides such as CaO, MgO, BaO, SrO, B_2O_3, P_2O_5, and Eu_2O_3. However, large-scale screening would take too long and be too expensive. It is therefore practically impossible to track down the whole space by a simple incremental searching methodology based on the high-throughput combinatorial screening. Even if a sparse mesh were employed, having a pitch on the surface edge approximately 0.1 mol, several hundred thousand samples would be necessary. It would not be possible to build such a large library, even with the most advanced experimentation system for high-throughput combinatorial screening. Therefore, it is necessary to employ a proper optimization strategy to avoid futile efforts and to achieve a systematic screening in our seven-dimensional parameter space. In particular, a good optimization strategy based on computational processes is definitely required.

* Corresponding author. E-mail: kssohn@sunchon.ac.kr.
[†] Sunchon National University.
[‡] Sangju National University.
[§] Pohang Accelerator Laboratory.

(1) Sohn, K.-S.; Cho, S. S.; Park, S. S.; Shin, N.; Weber, M. J. *Appl. Phys. Lett.* **2006**, *89*, 051106−1.
(2) Sohn, K.-S.; Yoo, J. G.; Shin, N.; Toda, K.; Zang, D.-S. *J. Electrochem. Soc.* **2005**, *152*, H213.
(3) Shin, N.; Kim, J.; Ahn, D.: Sohn, K.-S. *Acta. Crystallogr. C* **2005**, *61*, i54.
(4) Hoffman, M. V. *J. Electrochem. Soc.* **1968**, *115*, 560.
(5) Shionoya, S.; Yen, W. M. *Phosphor handbook*; CRC Press: Boca Raton, FL, 1999; pp 393−398.
(6) Yen, W. M.; Weber, M. J. *Inorganic Phosphors*; CRC Press: Boca Raton, FL, 2004; pp 87−90.

10.1021/cm070976b CCC: $37.00
Published on Web 10/04/2007

Table 1. Details about the Solutions Used in Precursor Delivery

metal compound	company providing compd	solvent	metal concentration
$Mg(NO_3)_2 \cdot 6H_2O$	Kojundo	deionized water	0.5 M
$Sr(NO_3)_2$	Aldrich	deionized water	0.5 M
$Ca(NO_3)_2 \cdot xH_2O$	Kojundo	deionized water	0.5 M
$Ba(NO_3)_2$	Kojundo	deionized water	0.25 M
H_3BO_3	Duksan	deionized water	0.5 M
$(NH_4)H_2PO_4$	Aldrich	deionized water	0.5 M
Eu_2O_3	Kojundo	deionized water + 10 mL of HNO_3	0.1 M

Several successful cases of material optimization have been reported in which new phosphors for use in plasma displays (PDP) and light-emitting diodes (LED) were found by using genetic algorithm-assisted combinatorial chemistry (GACC).[7−10] GACC is one of the most efficient global optimization strategies and is most compatible with high-throughput combinatorial chemistry experimentation. GACC has been successfully utilized for the development of inhomogeneous catalysts for the past few years.[11−13] However, GACC has rarely been adopted as a tool in the development of other inorganic functional materials. Only the present authors have used GACC to develop inorganic functional materials, except for the catalysts, i.e., inorganic phosphors for PDPs and LEDs. Inorganic phosphors may be more suitable for GACC in that the high-throughput characterization procedures appear much simpler than those for catalysts. Considering GACC achievement in the field of the catalyst and phosphor research,[7−13] it is apparent that GACC has proven to be very useful for materials development and for the design of experiments.

In the present investigation, GACC was utilized as a preliminary step prior to the final high-throughput screening process, which led to the identification of promising compositions. This implies that GACC acted as an early guide, elucidating the final direction to be exploited in the ensuing screening. The post-GACC high-throughput screening (referred to as fine-tuning), based on conventional quaternary and ternary combinatorial library techniques, was as significant as the GACC process in facilitating the whole optimization process and correctly identifying the optimum composition. The present investigation focused on the development of new materials of high performance (promising blue phosphors in this case) and on the full utilization of GACC and improvement in its performance.

2. Experimental Procedures

Eu^{2+}-doped $Eu_2O_3-SrO-CaO-BaO-MgO-B_2O_3-P_2O_5$ seven-dimensional combinatorial libraries were produced by a solution-based synthesis method based on the high-throughput screening

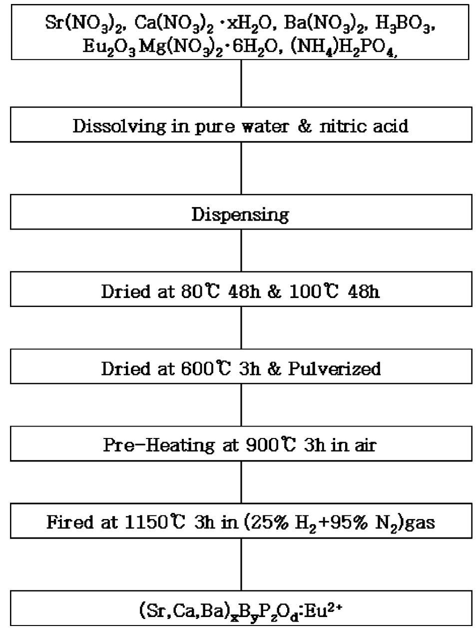

Figure 1. Flow chart of the sample preparation.

technique. All the law powders, europium oxide (Eu_2O_3), and calcium nitrate ($Ca(NO_3)_2$), such as strontium nitrate ($Sr(NO_3)_2$), barium nitrate ($Ba(NO_3)_2$), magnesium nitrate hydrous ($Mg(NO_3)_2 \cdot 6H_2O$), boric acid (HBO_3), and ammonium dihydrogen phosphate ($(NH_4)H_2PO_4$), were dissolved in deionized water or in dilute nitric acid. The details about the solutions used in the precursor delivery are summarized in Table 1.The correct amount of each solution was then injected into each sample site in 8 mL test tube arrays according to the composition table. The composition dealt with in the present investigation does not stand for the actual stoichiometry, but for the processing composition, unless otherwise described. The solutions in the test tube were then dried at 80−100 °C for 96 h and further dried at 600 °C for 6 h. The dried samples were pulverized and moved into a specially designed quartz glass container called a "combichem" container (or reactor). The dried samples were heated up to 900 °C for 3 h in the air and successively fired at 1150 °C in a reducing atmosphere. The reducing atmosphere was produced by introducing a mixture of nitrogen and a certain amount of hydrogen (25%) into the furnace so that the desired oxidation state of the activator ions Eu^{2+} could be achieved. Figure 1 shows a flow chart of the sample preparation. Previous reports have included more details about the combichem experiment.[14−20]

Some of the samples chosen from the library were removed from the combichem containers and examined by synchrotron X-ray diffraction (XRD) at Beamline 8C2 of the Pohang Light Source in Korea. The incident X-rays were vertically focused by a mirror and monochromatized to a wavelength of 1.5497 Å by a double bounce Si(111) monochromator. The monochromator also focused the X-rays horizontally. Momentum transfer resolution was con-

(7) Sohn, K.-S.; Park, D. H.; Cho, S. H.; Kwak, J. S.; Kim, J. S. *Chem. Mater.* **2006**, *18*, 1768.
(8) Sohn, K.-S.; Park, D. H.; Cho, S. H.; Kim, B. I.; Woo, S. I. *J. Comb. Chem.* **2006**, *8*, 44.
(9) Sohn, K.-S.; Lee, J. M.; Shin, N. *Adv. Mater.* **2003**, *15*, 2081.
(10) Sohn, K.-S.; Kim, B. I.; Shin, N. *J. Electrochem. Soc.* **2004**, *151*, H243.
(11) Buyevskaya, O. V.; Bruckner, A.; Kondratenko, E. V.; Wolf, D.; Baerns, M. *Catal. Today* **2001**, *67*, 369.
(12) Wolf, D.; Buyevskaya, O. V.; Baerns, M. *Appl. Catal., A* **2000**, *200*, 63.
(13) Paul, J. S.; Janssens, R.; Denayer, J. F. M.; Baron, G. V.; Jacobs, P. A. *J. Comb. Chem.* **2005**, *7*, 407.
(14) Sohn, K.-S.; Lee, J. M.; Jeon, I. W.; Park, H. D. *J. Electrochem. Soc.* **2003**, *150*, H182.
(15) Sohn, K.-S.; Lee, J. M.; Jeon, I. W.; Park, H. D. *J. Mater. Res.* **2002**, *17*, 3201.
(16) Kim, C. H.; Park, S. M.; Park, J. G.; Park, H. D.; Sohn, K.-S.; Park, J. T. *J. Electrochem. Soc.* **2002**, *149*, H21.
(17) Sohn, K.-S.; Jeon, I. W.; Chang, H.; Lee, S. K.; Park, H. D. *Chem. Mater.* **2002**, *14*, 2140.
(18) Seo, S. Y.; Sohn, K.-S.; Park, H. D.; Lee, S. *J. Electrochem. Soc.* **2002**, *149*, H12.
(19) Sohn, K.-S.; Seo, S. Y.; Park, H. D. *Electrochem. Solid State Lett.* **2001**, *4*, H26.
(20) Sohn, K.-S.; Park, E. S.; Kim, C. H.; Park, H. D. *J. Electrochem. Soc.* **2000**, *147*, 4368.

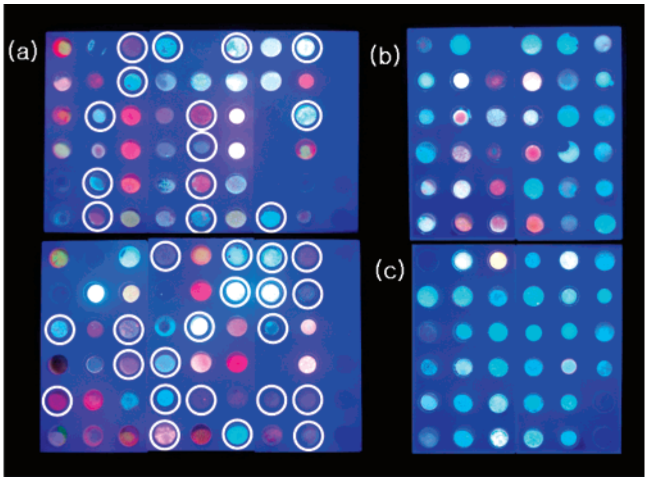

Figure 2. (a) Combichem library consisting of 96 samples at 254 nm excitation; 36 members marked by a circle represent the first generation in the GACC optimization process, (b) the second generation, and (c) the third generation.

trolled by two pairs of slits on the detector arm and was set at 0.001 Å^{-1} in this experiment. The emission spectra were monitored at 254 nm in a high-throughput manner, with the samples being left in the combichem containers using a plate reader accessory attached to a Perkin-Elmer LS50B spectrometer with a xenon flash lamp. The luminance was calculated by integrating the product of the emission spectrum and the standard visual spectral efficiency curve based on CIE (Commission Internationale de l'Eclairage) regulation.[21] The computation for the GACC optimization process was performed on the Microsoft visual basic platform.

3. Results and Discussion

3.1. GACC Process. Ninety-six (96) randomly chosen compositions in the Eu^{2+}-doped (Ca,Sr,Ba,Mg)$_x$B$_y$P$_z$O$_\delta$ system were synthesized by the high-throughput synthesis technique. Figure 2a shows 96 samples in the combichem reactor at 254 nm excitation—called the combichem library. A variety of emission colors were observed in the library, which is ascribed to the nature of 4f−5d transition of divalent europium. This reflects the fact that the emission peak position is strongly influenced by the local structure (crystal field) around the divalent europium ion. There are many melted glassy members in the library, and some members exhibit no luminescence. Some members were lost due to evaporation during either the drying or the firing process, accounting for some empty sites in the library. Such sample loss took place even in later generations. For this reason, the entire initial library could not be adopted as a starting generation in the GACC process. It is necessary to adopt a good quality initial library for a faster optimization process. Only 36 members were chosen by taking into account the luminance, the color chromaticity, and determination of whether they were melted. Through this elimination process, bad members were excluded and a promising starting generation was constituted for GACC. The selected members are marked by white circles in Figure 2a. The color chromaticity of this selected library was plotted in Figure 3a. The exact position of NTSC (National Television Standards Committee) blue was marked by a pentacle ($x = 0.14$, $y = 0.08$). The average distance (or deviation) from the point of NTCS blue in the chromaticity coordinates was 0.04439. The color chromaticity data of the first generation were spread widely but congested slightly toward the lower y region, wherein deep blue or purplish colors were obvious, as can be seen in Figure 2a. This implies that the selection process allowed many members around this area to survive.

The selected library was regarded as the first generation to be applied to the GACC optimization process. The deviation from the NTSC blue color in the chromaticity coordinates was set as an objective (cost or fitness) function to be minimized in the GACC process. In fact, it was not possible to take both the color chromaticity and luminescent efficiency into consideration simultaneously during the GACC optimization process. One promising way of dealing with the concurrent optimization of two or more properties of concern is to employ a multiobjective function. In principle, it is customary to introduce weighting factors into the multiobjective function for more systematic optimization. However, in the present optimization task there was no possible norm on which to develop a proper multiobjective function. In-depth considerations about objective function setting are outside the scope of the present investigation, which dealt only with the deviation from the NTSC blue point in the color chromaticity coordinates as a single-objective function.

Consequently, the deviation was minimized by genetic algorithm operations such as selection, crossover, and mutation. Details about the GACC process adopted in the present investigation are well-described in the literature.[7−10] Roulette wheel selection was adopted and the crossover and mutation rates were all set at 100%. Elitism was not adopted in the present GACC process because the population size was too small to allow for elitism. Instead of elitism, which amounts to letting well-known members occupy several sites in the next generation, new members were permitted to be generated in the next generation to enhance the possibility of obtaining better members of lower fitness, thereby allowing for more prominent refreshment. However, it is not clear whether skipping elitism had a positive influence on the evolution of the system. The single-point crossover was adopted and the crossover point was determined randomly. Mutation was achieved by adding and subtracting an arbitrary number (referred to as mutation number) below 0.05 mol for two arbitrarily chosen components. If the mole fraction of the chosen component were smaller than the mutation number, then the mutation number was replaced by the mole fraction of the component such that the chosen component vanished.

Figure 2b shows the second generation that resulted from the first generation after the above-described genetic operations. One member was lost during the preparation, which left a total of 35. Although there seemed to be no conspicuous improvement, the average fitness value (the deviation from the NTCS blue) was lowered slightly, to 0.04379. It might be controversial to argue that this small improvement (approximately 1%) resulted from the GACC optimization process. It should be noted, however, that Figure 2b shows

(21) Shionoya, S.; Yen, W. M. *Phosphor handbook*; CRC Press: Boca Raton, FL, 1999; pp 799−812.

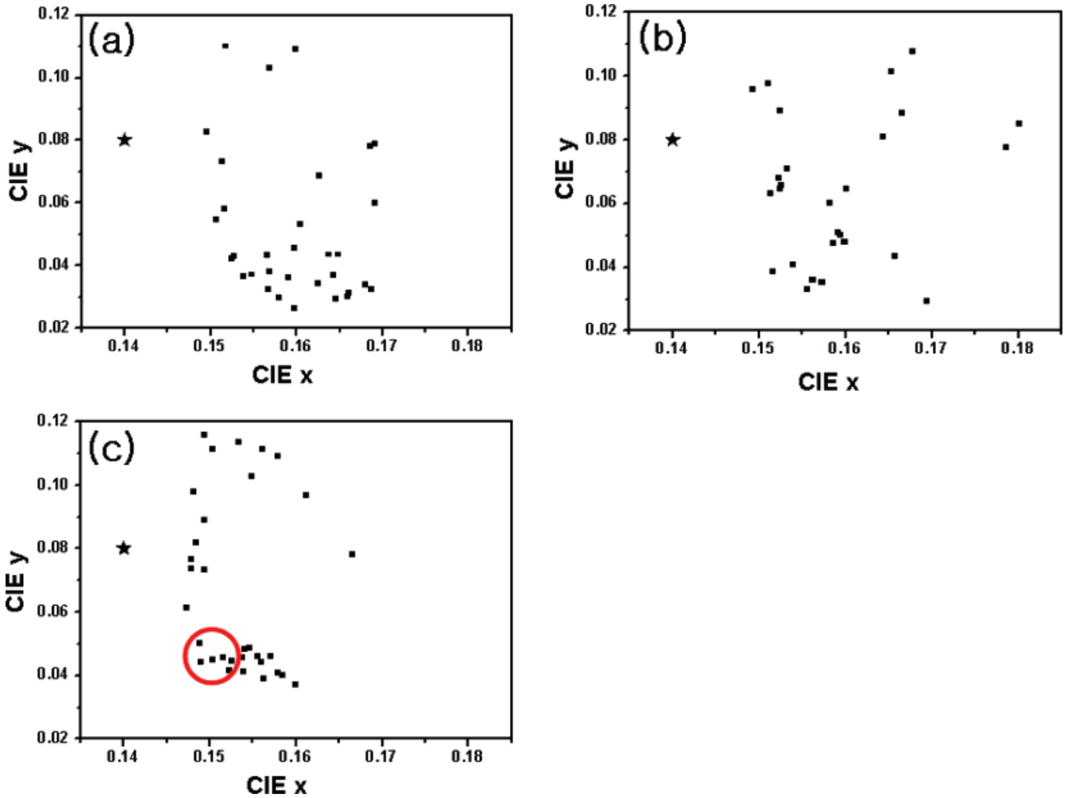

Figure 3. Color chromaticity diagrams of (a) the first generation, (b) the second generation, and (c) the third generation in the GACC optimization process, wherein a promising group is marked as a circle; the pentacle stands for the NTSC blue point.

redistribution in the chromaticity coordinates caused by the genetic operations, such that the first generation's congested data distribution in the low *y* region disappears, resulting in a more even distribution in the second generation. In addition, there appeared more bluish phosphors in the second generation, which was clearly detected in both the actual photograph and color chromaticity coordinates, as illustrated by Figure 2b and Figure 3b. The genetic operations were also applied to the second generation, thereby yielding the third. Figure 2c shows the third generation, wherein more bluish members appear. Three members in the third generation were discarded just after the drying process at 600 °C. Thus, they were excluded and a total of only 33 members were produced in the third generation. The average fitness value of the third generation was 0.03197. This value was reduced by more than 20% compared to the preceding generation. Although the decrease is partly attributed to the lost members, the decrease in the average fitness should be indicative of a certain degree of optimization taking place as a result of the GACC execution. Figure 3c shows that the redistribution of data also took place in the third generation, wherein a congested area in the low *y* region was again detected. This data congestion in the third generation appears to be similar to that of the first generation, but much narrower and also closer to the NTSC blue. It is also obvious that the congested region in the chromaticity coordinates of the third generation corresponded to fainter blue coloring, indicating an improved possibility of use in actual applications. The GACC process was stopped at the third generation.

In fact, the luminescent intensity was not the concern in the present GACC optimization process; only the color purity was of primary interest. It was found that high-luminescent intensity was obtained in the congested area mentioned above, in the low *y* region in the chromaticity coordinates, which was indicated by a circle in the third generation, illustrated by Figure 3c. It was expected that the luminance trend would be quite different from the luminescent intensity trend when the emission spectrum was positioned in the tail part of the spectral eye sensitivity curve, like either blue or red color emission, because the luminance was calculated by integrating the product of the emission spectrum and the standard visual spectral efficiency curve (spectral eye sensitivity curve) based on the CIE regulation.[21] The high *y* region in the chromaticity coordinates was found to be favorable in terms of luminance but the luminescent color was greenish, deviating far from the NTSC blue in the direction of reducing the color realization scope, so that the high *y* members cannot practically be used as a blue phosphor for any kind of application. Even if the deviation value were similar, the downward deviation would be more favorable in view of the color realization scope. Considering all aspects, such as color chromaticity, luminescent intensity, luminance, and even color realization scope, the members inside the circle in Figure 3c proved to be promising. These members should be scrutinized in planning for the next step, rather than making more generations according to the GACC sequences, because the present GACC process, implemented only in terms of color chromaticity, has limitations in other aspects, such as luminescent intensity, luminance, and color realization scope. Therefore, no prominent improvement would have been feasible by running the GACC process further. This was also supported by the fact that the members closer to the NTSC blue point in the medium *y* region, which

Table 2. Processing Compositions and Color Chromaticity *x,y* Values of the Six Finally Selected Members inside the Circle in Figure 3c

sample	Eu	Mg	Ca	Sr	Ba	B	P	CIE$_x$	CIE$_y$
1	0.005	0.000	0.199	0.217	0.000	0.186	0.392	0.1523	0.0415
2	0.005	0.000	0.229	0.144	0.043	0.182	0.397	0.1526	0.0445
3	0.004	0.000	0.304	0.113	0.000	0.186	0.392	0.1489	0.0441
4	0.005	0.030	0.192	0.131	0.054	0.218	0.370	0.1503	0.0449
5	0.005	0.034	0.201	0.108	0.089	0.210	0.354	0.1515	0.0457
6	0.004	0.035	0.210	0.105	0.054	0.221	0.370	0.1488	0.0502

could have been promising in terms of color chromaticity, exhibited too low luminescent intensity and luminance values to be considered practical. Accordingly, it would be advisable to quit at the third generation.

The exact compositions, along with the color chromaticity *x*,*y* values, of the members inside the circle are shown in Table 2. When the sum of alkali earth metal fractions was compared with the boron and phosphorus content, the integer set closest to those figures was 6:2:5. This integer set was found to be consistent with the processing composition adopted to achieve the complete synthesis of $Sr_6BP_5O_{20}:Eu^{2+}$ (SBP) phosphors.[1−3] In particular, when considering the relative portion of alkali earth metals, it was apparent that Mg and Ba contents were negligible and Ca and Sr contents were high. The XRD patterns of the members in Table 2 were indistinguishable. A representative XRD pattern of sample 3 in Table 2 will be presented in Figure 8, and more detailed explanations regarding the XRD result of sample 3 will be discussed in the next subsection. In spite of the findings described so far, a more systematic investigation was required for further improvements and better understanding. To this end, fine-tunings based on the final GACC results were implemented. A series of conventional high-throughput combinatorial screenings were carried out by referring to the GACC results as a basis for further library constructions. Only the alkali earth elements were varied, with the basic ratio 6:2:5 fixed using the quaternary and ternary libraries. Details of the fine-tuning screening will be discussed in the next subsection.

3.2. Fine-Tuning Using Quaternary and Ternary Screening. Figure 4a−c shows quaternary libraries in terms of luminance and CIE chromaticity *x* and *y*, respectively. The quaternary library consists of five shells including 121 compositions in the Eu^{2+}-doped $(Sr,Ca,Ba,Mg)_6B_2P_5O_\delta$ system. The Eu^{2+}-doping content was fixed to be a 1 mol % of total sum of alkali earth metals, which was adopted by referring to the GACC results in Table 2. The apex composition of each shell was presented in the table below the graphics. It is noted that the brighter the sphere, the higher the property of concern. This leads to the criterion that brighter spheres should be pursued in the luminescent library, whereas darker spheres should be favorable in the color chromaticity libraries, wherein *x* spans from 0.1475 to 0.2609 and *y* from 0.0353 to 0.2784. When luminance and CIE chromaticity *x* and *y* were taken into account, the Sr−Ca−Ba ternary area of the outermost shell appeared to be promising and deserving of further investigation. This decision was also consistent with the previous finding resulting from the GACC optimization process. The Sr−Ca−Ba surface of the outermost shell was separated and is shown on the right side of Figure 4a−c.

A more precise $(Ca,Sr,Ba)_6B_2P_5O_\delta:Eu^{2+}$ ternary library was also obtained in terms of luminance and CIE chromaticity *x* and *y*, as can be seen in Figure 5a−c. The actual library, photographed under 254 nm excitation, is shown in Figure 5d. The reason the high Sr region in the luminance library appears promising is that the typical SBP's greenish blue emission peaking at around 475 nm promoted the luminance value when the luminance was calculated by incorporating the standard visual spectral efficiency curve.[1−3] A similar feature was also observed in the quaternary luminance library, but this high luminance is not desirable in constituting a realistic blue color. The area enclosed by a small triangle in the libraries deserved to be fine-tuned in consideration of both luminance and color chromaticity. The relative luminance of some members in this enclosed region, especially the left side of the triangle, was around 70% of a commercially available BAM phosphor (NICHIA Co. Ltd.), and the color chromaticity *x* and *y* was estimated to be 0.15 ± 0.01 and 0.05 ± 0.005, respectively. The fine-tuning was implemented so that the small triangular region was zoomed in to achieve a more precise screening. Figure 6a−c shows the fine-tuned ternary libraries of luminance and color chromaticity. The actual library, photographed at 254 nm excitation, is shown in Figure 6d. Most members in this library exhibited promising quality in terms of luminance and color chromaticity, so it could be concluded that the final optimization process was completed. In particular, the area marked as an ellipsoid in Figure 6a was found to be the most promising composition range in terms of luminance—three representative compositions were also obtained in this area, marked by arrows. The exact processing compositions of these samples are $(Ca_{0.72}Sr_{0.24}Ba_{0.04})_6B_2P_5O_\delta:Eu^{2+}$, $(Ca_{0.64}Sr_{0.32}Ba_{0.04})_6B_2P_5O_\delta:Eu^{2+}$, and $(Ca_{0.52}Sr_{0.44}Ba_{0.04})_6B_2P_5O_\delta:Eu^{2+}$, which will be referred to as samples 5, 12, and 30, respectively. It is, of course, obvious that the color chromaticity of these promising samples was also acceptable, centering around a point $x = 0.15$, $y = 0.05$ and exhibiting a blue color emission. The compositions of these samples were close to those that resulted from the GACC optimization process presented in Table 2.

Figure 7a,b shows the emission spectra and color chromaticity data of samples 5, 12, and 30, together with data from a commercially available BAM phosphor. It was reconfirmed that the luminance of samples 5, 12, and 30 was 72, 74, and 74% of the BAM phosphor, respectively. It should be noted that the luminance is not comparable to the BAM phosphor, even though the luminescent intensity looked much higher than the BAM phosphor. Notwithstanding the lower luminance, this phosphor would have potential as a blue phosphor for use in cold cathode fluorescent lamps (CCFL) for the back light unit (BLU) of liquid crystal displays (LCD), if the luminance were improved slightly by controlling some extrinsic properties such as powder shape and size distribution. In addition, it should be noted that the color chromaticity deviates slightly from the NTSC blue. However, the deviation was downward from the NTSC blue point in the color chromaticity diagram and it still resided

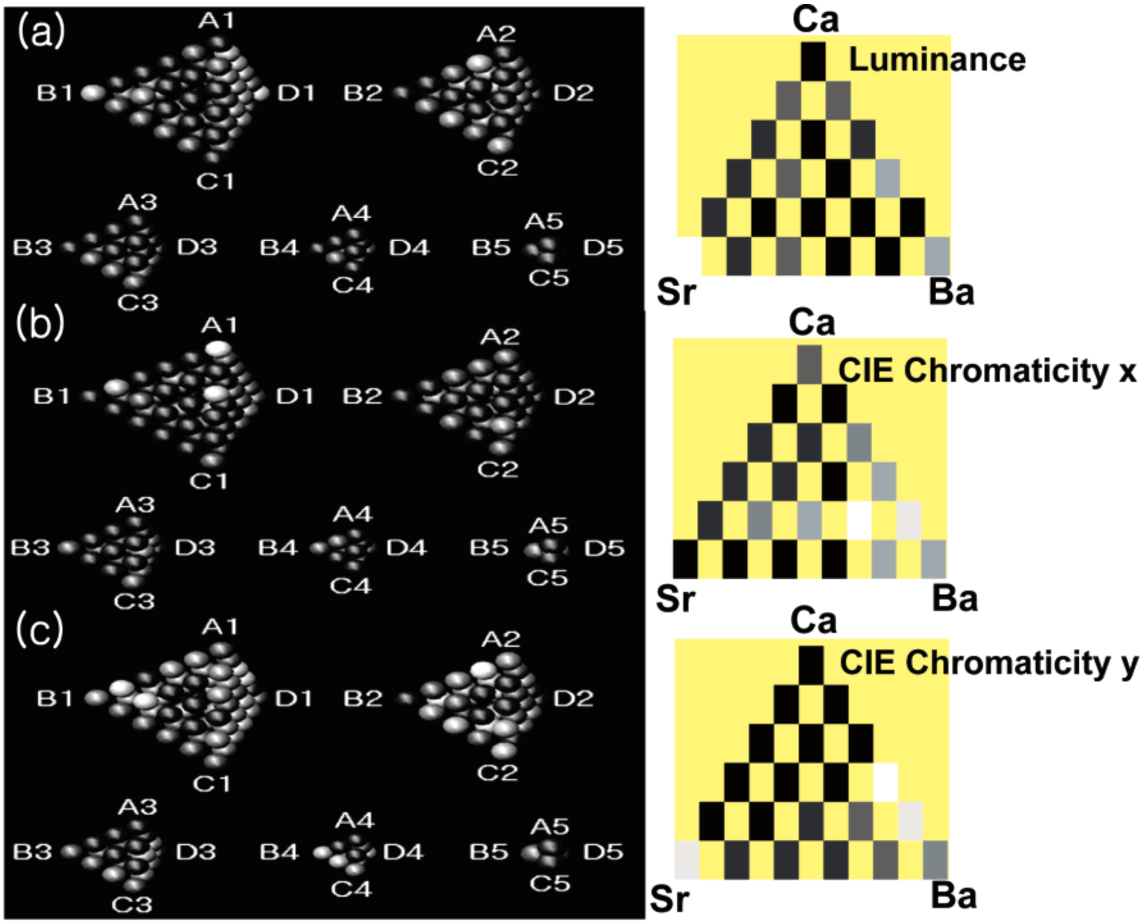

	1	2	3	4	5
A	$Mg_6B_2P_5O_\delta$	$(Mg_{0.825}Ca_{0.055}Sr_{0.055}Ba_{0.055})_6B_2P_5O_\delta$	$(Mg_{0.66}Ca_{0.11}Sr_{0.11}Ba_{0.11})_6B_2P_5O_\delta$	$(Mg_{0.495}Ca_{0.165}Sr_{0.165}Ba_{0.165})_6B_2P_5O_\delta$	$(Mg_{0.33}Ca_{0.22}Sr_{0.22}Ba_{0.22})_6B_2P_5O_\delta$
B	$Sr_6B_2P_5O_\delta$	$(Mg_{0.055}Ca_{0.055}Sr_{0.825}Ba_{0.055})_6B_2P_5O_\delta$	$(Mg_{0.11}Ca_{0.11}Sr_{0.66}Ba_{0.11})_6B_2P_5O_\delta$	$(Mg_{0.165}Ca_{0.165}Sr_{0.495}Ba_{0.165})_6B_2P_5O_\delta$	$(Mg_{0.22}Ca_{0.22}Sr_{0.33}Ba_{0.22})_6B_2P_5O_\delta$
C	$Ca_6B_2P_5O_\delta$	$(Mg_{0.055}Ca_{0.825}Sr_{0.055}Ba_{0.055})_6B_2P_5O_\delta$	$(Mg_{0.11}Ca_{0.66}Sr_{0.11}Ba_{0.11})_6B_2P_5O_\delta$	$(Mg_{0.165}Ca_{0.495}Sr_{0.165}Ba_{0.165})_6B_2P_5O_\delta$	$(Mg_{0.22}Ca_{0.33}Sr_{0.22}Ba_{0.22})_6B_2P_5O_\delta$
D	$Ba_6B_2P_5O_\delta$	$(Mg_{0.055}Ca_{0.055}Sr_{0.055}Ba_{0.825})_6B_2P_5O_\delta$	$(Mg_{0.11}Ca_{0.11}Sr_{0.11}Ba_{0.66})_6B_2P_5O_\delta$	$(Mg_{0.165}Ca_{0.165}Sr_{0.165}Ba_{0.495})_6B_2P_5O_\delta$	$(Mg_{0.22}Ca_{0.22}Sr_{0.22}Ba_{0.33})_6B_2P_5O_\delta$

Figure 4. $(Ca,Sr,Ba,Mg)_6B_2P_5O_\delta:Eu^{2+}$quaternary libraries in terms of (a) luminance and CIE chromaticity (b) *x* and (c) *y*; the Sr−Ca−Ba surfaces of the outermost shell are presented separately on the right side.

in the blue color range. In this regard, as far as the color realization scope was concerned, it would even be possible to argue that samples 5, 12, and 30 are more favorable than the BAM phosphor.

After completion of the optimization process involving GACC, and the ensuing quaternary/ternary screening, the next step was the structural examination of the resulting phosphors. To this end, XRD patterns of four representative phosphors were examined. Sample 3 resulted from the GACC process, which is identified in Table 2, and samples 5, 12, and 30 were obtained from the final ternary library in Figure 6a. Figure 8 shows their XRD patterns. All the XRD patterns were identical and also matched well with the standard pattern of $Sr_2P_2O_7$ (referred to as "SP") from the Joint Committee on Powder Diffraction Standards (JCPDS). It was clearly confirmed that the samples were crystallized into the SP structure (space group *Pnma*, No. 62). The considerable boron content in the samples mattered most because it was not detectable in the XRD measurement, as shown in Figure 8. The overall feature of the sample patterns was analogous to the standard data, but the peak locations did not exactly coincide with the standard data. Accordingly, it is reasonable to argue that the samples crystallized in the SP structure, although a certain amount of calcium and barium was dissolved into the structure by substituting for strontium, and that the boron content was evaporated during the firing as it was acting as a fluxing agent. However, it is not clear whether or not boron just acted as a fluxing agent.

Energy dispersive spectroscope (EDS) analysis revealed that boron was not detected at all in the final samples (samples 5, 12, and 30), even though a considerable amount of boron was included in the initial solutions. Boron or boron-containing compounds should be evaporated not only in the firing process at high temperature around 900−1200 °C but also in the drying process of liquid solution at much lower

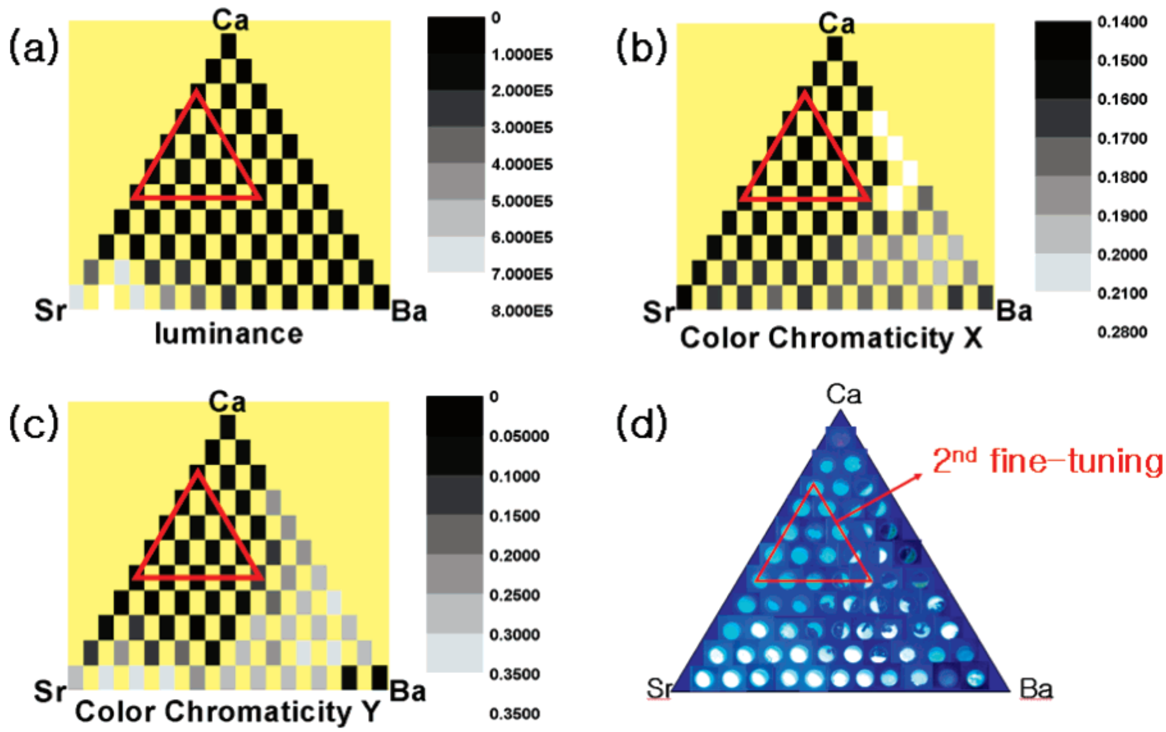

Figure 5. (Ca,Sr,Ba)$_6$B$_2$P$_5$O$_\delta$:Eu^{2+} ternary library in terms of (a) the luminance and the CIE chromaticity (b) *x*, (c) *y*, and (d) the actual library photographed under 254 nm excitation; the small triangle on the library designates the selected region to be fine-tuned.

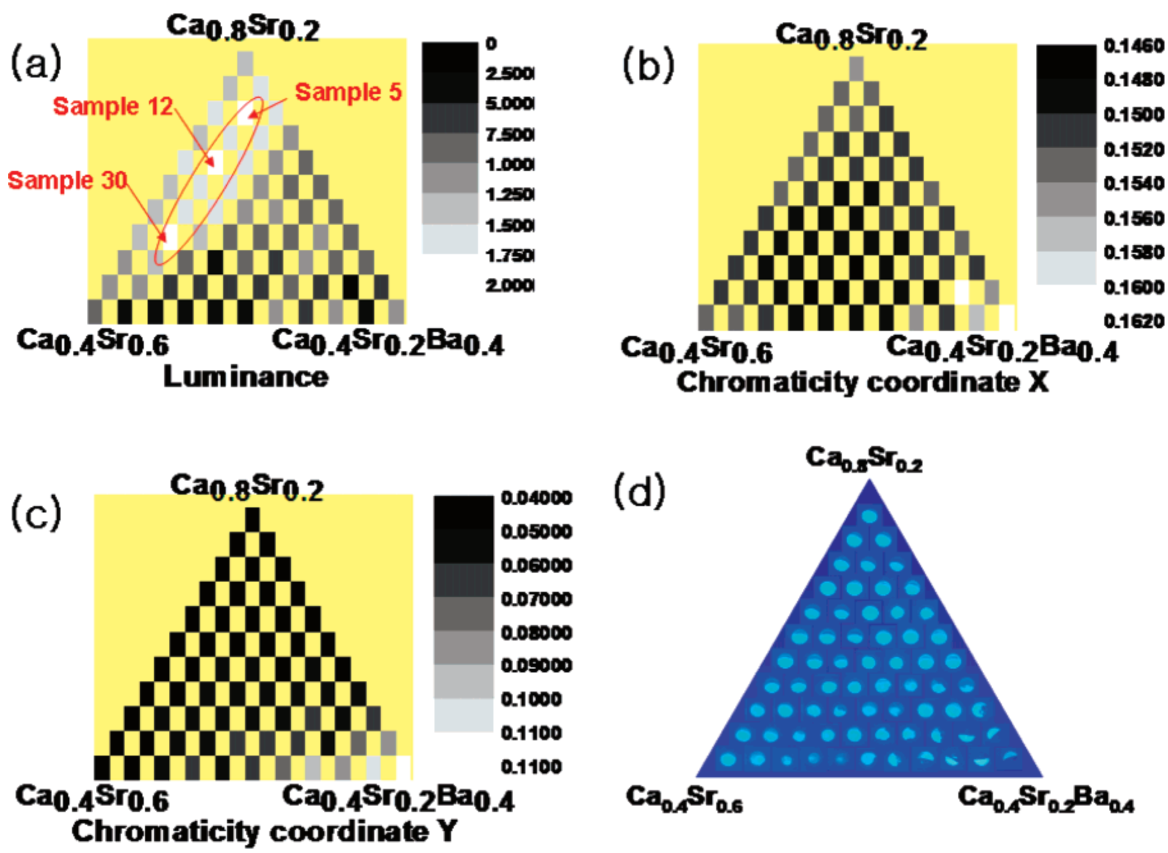

Figure 6. Fine-tuning of the selected region from the (Ca,Sr,Ba)$_6$B$_2$P$_5$O$_\delta$:Eu^{2+} ternary library in terms of (a) luminance and CIE chromaticity (b) *x*, (c) *y*, and (d) the actual library photographed under 254 nm excitation.

temperatures. So we eventually found that the depletion of boron was taking place all over the entire process. It is an interesting finding that boron was not detected in both EDS and XRD measurements, despite the fact that such a huge amount of boron was included in the initial solution. So this result was double-checked by two different EDS equipments. It was confirmed that our final samples contain no boron in the final structure but the inclusion of boron in the initial processing stage was of great help in enhancing the luminescence.

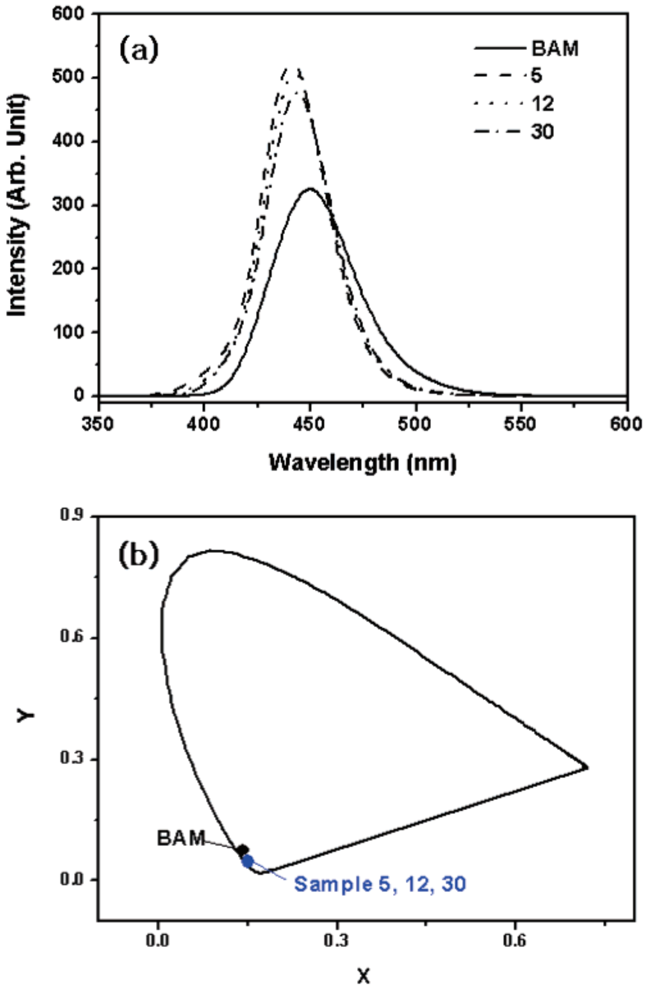

Figure 7. (a) Emission spectra and (b) color chromaticity data of samples 5, 12, and 30, together with data from a commercially available BAM phosphor.

Table 3. Compositions of Samples 5, 12, and 30 Estimated from the EDS Analysis; Four Different Locations Were Examined for Each Sample

sample	Eu	Ca	Sr	Ba	B	P	O
5	0.29	10.03	9.84	0.82	0	20.52	58.5
5	0.29	9.29	5.02	1.49	0	19.93	63.98
5	0.28	12.51	6.56	0.65	0	21.46	58.54
5	0.19	14.34	5.23	1.02	0	18.98	60.24
12	0.29	11.00	3.59	0.82	0	14.69	69.61
12	0.16	10.64	7.98	0.57	0	17.91	62.74
12	0.50	9.29	8.24	0.80	0	15.16	66.01
12	0.14	8.87	4.96	0.67	0	15.29	70.07
30	0.15	7.33	5.84	0.71	0	16.67	69.3
30	0.24	9.31	8.51	0.83	0	18.02	63.09
30	0.25	7.50	6.56	0.73	0	14.24	70.72
30	0.3	7.65	7.89	0.78	0	14.81	68.58

The EDS results are summarized in Table 3. The EDS results were in relatively good agreement with the processing compositions except for the fact that boron was completely missing. It is generally known that the EDS is powerful for a rough measure of composition, and also very useful when judging whether a certain element is present or absent, but it is common sense that the quantitative analysis of relative composition from EDS analyses is not 100% correct. Therefore, we expressed the final composition as a reasonable range instead of a definite composition. The final promising composition range was then proposed to be $(Sr_{1-x-y}Ca_xBa_y)_2P_2O_7:Eu^{2+}$ ($0.32 < x < 0.72$, $y < 0.04$).

In relation to the boron addition, a confirmatory experiment was done, wherein a similar quaternary library was synthesized but a remarkable distinction was the absence of boron, indicating that a $(Ca,Sr,Ba,Mg)_2P_2O_7:Eu^{2+}$quaternary library was constructed. The results from this auxiliary experiment are not presented here for the sake of brevity, but Supporting Information including these results is provided at the journal's web site. It was found that identical emission spectra were observed between the boron-incorporated and -excluded samples as far as the alkali earth element composition was similar, and also that the samples used for the comparison were identified to be the SP structure regardless of whether boron was present or absent. It should be noted, however, that the luminance of boron-excluded samples was much lower than that of boron-incorporated samples, reaching only 68% at best. This finding led to the conclusion that the boron was not dissolved into the SP structure but played an efficient role during the synthesis and in turn enhanced the luminance of samples. In addition to the boron addition, the alkali earth metal/phosphorus ratio (A/P) played a decisive role in achieving well-crystallized SP structure and in turn high luminescent efficiency. In fact, our optimized A/P ratio (6/5) was obtained from the GACC process, which slightly deviated from the exact stoichiometry value (A/P = 1). The samples with this inexact A/P ratio were much more promising in terms of luminance, indicating that the exact A/P ratio samples were not properly synthesized. The results from the A/P ratio experiment were also included in the Supporting Information file.

It is well-known that the $Sr_2P_2O_7:Eu^{2+}$ phosphor has an emission spectrum peaking at around 420 nm.[2,6] It should be noted that the phosphor, exhibiting an emission peak at around 420 nm, is completely useless for use in general displays and lightings, but available only for very limited applications such as an early photocopy machine.[6] Referring to the discussion regarding the high strontium region of the boron-containing ternary library in Figure 5a, it is clear that boron addition had a significant effect on the structure alteration in the high strontium region, such that the boron incorporation in the high strontium region converted the SP structure into the $Sr_6BP_5O_{20}:Eu^{2+}$ (SBP) structure. Such a structural change did not take place when the calcium and barium content exceeded a certain level, which might be the solubility limit of the SBP structure for the accommodation of the other alkali earth elements. The solubility limit of SBP structure was found to be about 20% for calcium and slightly higher for barium. It was found that there were no boron-containing structures in the $(Ca,Sr,Ba)_6B_2P_5O_\delta:Eu^{2+}$ ternary library other than the SBP structure. This finding confirms that the boron-involved structure was not allowed outside the high Sr region, and that the boron inclusion was just presumed to be served as a flux, which enhanced the crystallinity and powder properties and eventually promoted luminance. Figure 9 shows a succinct schematic showing the SBP-forming region and the desirable blue phosphor-forming region in the $(Ca,Sr,Ba)_6B_2P_5O_\delta:Eu^{2+}$ ternary library.

As mentioned above, the extremely deep blue emission of the $Sr_2P_2O_7:Eu^{2+}$ phosphor has narrowed the applicability

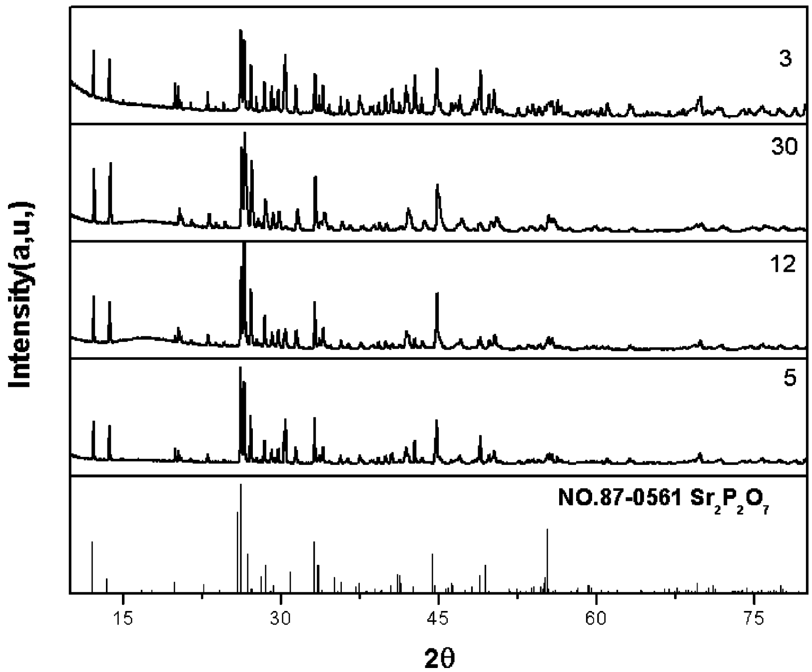

Figure 8. XRD patterns of sample 3, resulting from the GACC process, and samples 5, 12, and 30 obtained from the final ternary library.

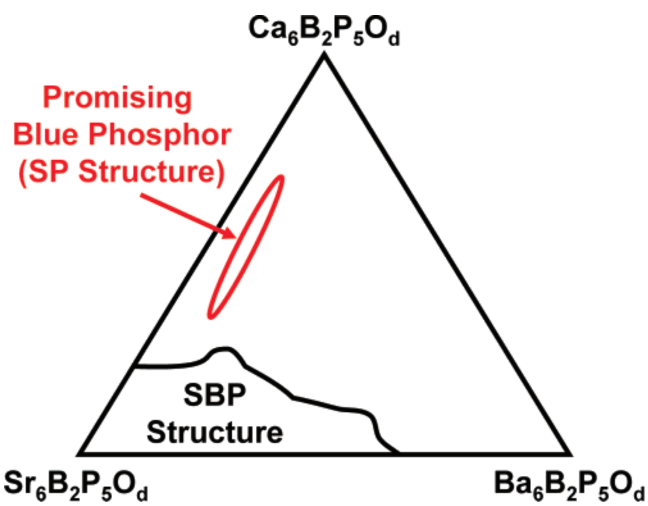

Figure 9. Schematic showing the SBP-forming region and the desirable blue phosphor-forming region

of this phosphor. In contrast to the conventional $Sr_2P_2O_7$:Eu^{2+} phosphor, samples 5, 12, and 30 exhibited an emission peak at 441−444 nm. The red shift of more than 20 nm was considered to be due to the other alkali earth element inclusions, especially calcium. Since the 4f−5d transition of divalent europium ions is greatly influenced by the crystal field,[22] it is reasonable for a small change in the local structure of Eu^{2+} activators to give rise to a considerable spectral change. It is still unclear how the calcium and barium inclusion altered the local structure around the divalent europium in the SP structure without long-range structural change, and in turn how it made the red shift in the emission spectrum. However, it was confirmed by the XRD, EDS, and PL data that the calcium and barium certainly resided in the SP structure and this inclusion played a significant role in improving color chromaticity by causing a considerable red shift. In this context, even though the starting compositions (so-called processing compositions) of samples 5, 12, and 30 were $(Ca_{0.72}Sr_{0.24}Ba_{0.04})_6B_2P_5O_\delta$:$Eu^{2+}$, $(Ca_{0.64}Sr_{0.32}Ba_{0.04})_6B_2P_5O_\delta$:$Eu^{2+}$, and $(Ca_{0.52}Sr_{0.44}Ba_{0.04})_6B_2P_5O_\delta$:$Eu^{2+}$, the correct, actual stoichiometries were believed to be $(Sr_{1-x-y}Ca_xBa_y)_2P_2O_7$:$Eu^{2+}$ ($0.32 < x < 0.72$, $y < 0.04$).

(22) Blasse, G.; Grabmaier, B. C. *Luminescent Materials*; Springer-Verlag: New York, 1994; pp 34−70.

4. Conclusions

The GACC process, followed by conventional high-throughput screenings, was useful for attaining a thorough optimization in the multicomposition system. We applied this methodology to the search for promising blue phosphors in the Eu^{2+}-doped (Ca,Sr,Ba,Mg)$_x$B$_y$P$_z$O$_\delta$ system and found promising blue phosphors, in the actual composition range of $(Sr_{1-x-y}Ca_xBa_y)_2P_2O_7$:$Eu^{2+}$ ($0.32 < x < 0.72$, $y < 0.04$). Their luminance was as high as 70% of a commercially available BAM phosphor at 254 nm excitation, and the color chromaticity was $x = 0.15 \pm 0.01$, $y = 0.05 \pm 0.005$. The GACC optimization process was proven to be an efficient, preliminary step to provide guidance for the final optimization by conventional high-throughput screening based on quaternary and ternary library techniques.

The XRD and EDS examination revealed the phosphors to be of SP structure, thereby suggesting that their real stoichiometries should be $(Sr_{1-x-y}Ca_xBa_y)_2P_2O_7$:$Eu^{2+}$ ($0.32 < x < 0.72$, $y < 0.04$). Their luminescent property was far better than the $Sr_2P_2O_7$:Eu^{2+} phosphor in terms of luminance and color chromaticity, which was explained by the fact that the solid solution of alkali earth elements in the SP structure enhanced the color chromaticity by slight alterations in the local structure around Eu^{2+} ions and that boron inclusion promoted luminance significantly while the boron completely escaped during the synthesis process.

The new phosphors developed in the present investigation deserve to be compared to well-known BAM and $Sr_5(PO_4)_3$-

Cl:Eu^{2+} phosphors in view of their promising luminescent properties. In this regard, $(Sr_{1-x-y}Ca_x Ba_y)_2P_2O_7$:$Eu^{2+}$ ($0.32 < x < 0.72$, $y < 0.04$) phosphors could be used as a substitute for these well-known commercially available blue phosphors, especially for use in cold cathode fluorescent lamps (CCFL) for liquid crystal display back light units (LCDBLU).

Acknowledgment. This work was supported by the Korea Research Foundation Grant funded by the Korean Government (MOEHRD, Basic Research Promotion Fund) (KRF-2006-D00121 - I00341).

Supporting Information Available: Quaternary library of luminance, comparison between boron-containing and -excluding samples, effect of A/P ratio on synthesis with boron addition, and experimental consistency (PDF). This material is available free of charge via the Internet at http://pubs.acs.org.

CM070976B